Hindawi
Scientific Programming
Volume 2023, Article ID 9865218, 1 page
https://doi.org/10.1155/2023/9865218

Retraction

Retracted: An Intelligent Evaluation Method of Information Course Teaching Effect Based on Image Analysis

Scientific Programming

Received 8 August 2023; Accepted 8 August 2023; Published 9 August 2023

This article has been retracted by Hindawi following an investigation undertaken by the publisher [1]. This investigation has uncovered evidence of one or more of the following indicators of systematic manipulation of the publication process:

(1) Discrepancies in scope
(2) Discrepancies in the description of the research reported
(3) Discrepancies between the availability of data and the research described
(4) Inappropriate citations
(5) Incoherent, meaningless and/or irrelevant content included in the article
(6) Peer-review manipulation

The presence of these indicators undermines our confidence in the integrity of the article's content and we cannot, therefore, vouch for its reliability. Please note that this notice is intended solely to alert readers that the content of this article is unreliable. We have not investigated whether authors were aware of or involved in the systematic manipulation of the publication process.

Wiley and Hindawi regrets that the usual quality checks did not identify these issues before publication and have since put additional measures in place to safeguard research integrity.

We wish to credit our own Research Integrity and Research Publishing teams and anonymous and named external researchers and research integrity experts for contributing to this investigation.

The corresponding author, as the representative of all authors, has been given the opportunity to register their agreement or disagreement to this retraction. We have kept a record of any response received.

References

[1] H. Chen and J. Zhang, "An Intelligent Evaluation Method of Information Course Teaching Effect Based on Image Analysis," *Scientific Programming*, vol. 2021, Article ID 3200865, 9 pages, 2021.

Hindawi
Scientific Programming
Volume 2021, Article ID 3200865, 9 pages
https://doi.org/10.1155/2021/3200865

Research Article

An Intelligent Evaluation Method of Information Course Teaching Effect Based on Image Analysis

HaiDong Chen[1] **and JuFang Zhang**[2]

[1]*Dean's Office, Shang Hai East Sea College, Shang Hai 201206, China*
[2]*Dean's Office, Shang Hai Jiao Tong University, Shang Hai 200241, China*

Correspondence should be addressed to HaiDong Chen; 1168@esu.edu.cn

Received 22 September 2021; Revised 18 October 2021; Accepted 25 October 2021; Published 8 November 2021

Academic Editor: Bai Yuan Ding

Due to its own limitations, the traditional teaching quality evaluation method has been unable to adapt to the development of information-based curriculum teaching. Therefore, the establishment of a scientific and intelligent teaching effect evaluation method will help to improve the teaching quality of college teachers. To solve the above problems, a student fatigue state evaluation method based on the quantum particle swarm optimization artificial neural network is proposed. Firstly, face detection is realized by adding three Haar-like feature blocks and improving the AdaBoost algorithm of a weak classifier connection. Secondly, in order to effectively improve the image imbalance, the MSR algorithm is used to enhance the face data image, which is effectively suitable for network training. Then, by readjusting the connection mode, the DenseNet is improved to fully reflect the local detail feature information of the low level. Finally, quantum particle swarm optimization (QPSO) is used to optimize the DenseNet structure, which makes the optimization of network structure more automatic and solves the uncertainty of manual selection. The experimental results show that the proposed method has a good detection effect and prove the effectiveness and correctness of the proposed method.

1. Introduction

With the rapid development of Educational Informatics, it has been widely used in many aspects of the higher education field and achieved good results, but research and practice have lagged behind in measuring teaching quality, such as the teaching quality evaluation system and evaluation model; it is well known that the evaluation of teaching quality analysis is a very complex nonlinear process [1–4]; there are multiple influencing factors and dynamic variables involved, so that the traditional model of the teaching quality has become less fully competent in work addressing this ambiguity.

At present, cameras are used in most classrooms of information courses to monitor students' status in real time, resulting in a large amount of video data. The traditional teaching quality evaluation method needs to monitor each student's sitting posture, facial expression, and other information in the video manually to judge whether each student has fatigue. This method has the problems of low efficiency and high labor cost [5–8], so it cannot be popularized and applied on a large scale. How to find the fatigue state of students in time and effectively by means of automation in practical application, so as to effectively prevent the occurrence of students' inattention in class, has a strong practical significance and helps to ensure the teaching quality of information-based courses.

Artificial intelligence uses computers to simulate some human thinking processes and intelligent behaviors, so as to endow machines with human intelligence [9–11]. Machine learning is a branch of artificial intelligence, and its most successful application is in the field of computer vision [12, 13]. As a technology to realize machine learning, deep learning has attracted great attention. Deep learning adopts a multilevel network structure to model the human brain autonomous learning. The advantages of deep learning are

mainly in the following two aspects. First, deep learning mostly adopts a deep neural network. With the deepening of network level, it can often get better learning effect, which is far from being achieved by shallow learning [14, 15]. Second, in-depth learning attaches great importance to the learning of the characteristics of the training object and has a very strong feature learning ability [16–18]. Many researchers have applied deep learning to fatigue state detection tasks and achieved good recognition accuracy, among which the most representative is the artificial neural network. However, the essence of the artificial neural network is a gradient descent algorithm, which will fall into a local optimal solution. Theoretically, it still has room for optimization.

In order to solve the above problems, this study proposed a student fatigue state evaluation method based on the quantum particle swarm optimization artificial neural network. The proposed method improves DenseNet [19] by reducing the number of redundant connections, so as to fully reflect low-level local detail feature information. Finally, QPSO [20] is used to optimize the DenseNet structure and increase the number of hyperparameters, which makes the optimization of network structure more automatic and solves the uncertainty problem of artificial selection. Experimental results show that, on CAS_PEAL and self-built datasets, the accuracy of the QPSO-DenseNet algorithm is higher than that of the optimal DenseNet structure selected manually.

2. Literature Review

For students in the information class, physical fatigue will lead to distraction, leading to students being unable to concentrate in the normal teaching process. The research technology on fatigue state detection at home and abroad began in the 1930s and has not made great progress. It is not until the last two decades that the research results have made great progress, which is mainly due to the development of information processing technology, sensor technology, and deep learning technology in recent years. Research on fatigue state detection can be divided into two aspects: the method based on physiological parameters and the method based on human behavior characteristics.

The fatigue state detection method based on physiological parameters receives signals from electrode patches on the forehead, heart, and muscle through medical special instruments and equipment, and the signals are transmitted to the system for real-time analysis. The threshold value of physiological parameter signals defined clinically is used as the basis for fatigue discrimination. Luo et al. [21] evaluated driving fatigue based on frontal EEG signals. Wang et al. [22] proposed the method of deep learning and convolution neural network combined with EEG, which improved the detection accuracy compared with previous methods. However, physiological parameters are mostly collected by special human body signal acquisition instruments, and the volume of medical equipment is relatively large, which cannot be used in the classroom. In addition, because one end of the data acquisition equipment must be connected to the skin of the human body, it is not conducive to normal teaching activities, so the adaptability is poor.

The driver fatigue state detection method based on driver behavior characteristics is a research method combining pattern recognition and image processing technology. With the facial state image collected with the camera as the input data, after image processing and computer vision-related technology processing, the dynamic data of the eyes and mouth on the face are analyzed to judge whether the fatigue limit is reached and then the fatigue state is judged. At present, there are many research results using this method. Qian et al. [23] used Haar-like features and AdaBoost classifier to conduct real-time detection of the face and analyzed the optimal sampling rate and minimum possible target size to improve detection accuracy and calculation efficiency. Eye localization and iris localization are performed on the detected face. Finally, PERCLOS was used as the criterion to judge fatigue. You et al. [24] used elliptic curve fitting and image enhancement methods, respectively, to determine fatigue according to eye opening. Guo et al. [25] used the convolutional neural network and Bayesian network, respectively, to extract face features and the relationship between features.

In order to improve the accuracy of student fatigue state evaluation, this paper proposes a student fatigue state evaluation method based on the quantum particle swarm optimization artificial neural network. Firstly, face detection is realized by the improved AdaBoost algorithm. Secondly, in order to effectively improve the image imbalance, Multiscale Retinex (MSR) [26] algorithm is used to enhance the face data image. Then, DenseNet is improved by reducing the number of redundant connections. Finally, the DenseNet structure was optimized by QPSO.

3. Evaluation Method of Students' Fatigue State

3.1. Face Detection Based on the Improved AdaBoost Classifier. The purpose of this stage of face detection is to determine the position of the human face region in the whole image from the input image and output coordinates and other information, such as head tilt angle. Face detection is a key step in the study of student fatigue state detection. Although the relative positions of facial features are roughly the same, it is still very difficult to detect faces under the influence of different expressions and external light.

In the face detection stage, the cascaded AdaBoost classifier [27] can quickly exclude a large number of nonface images at the initial stage of training, which will greatly help improve the efficiency of face detection in the end. Haar-like features are inspired by Haar wavelet transform, which can describe feature edges and feature changes in each direction of the image in detail. Haar-like feature is an important tool for AdaBoost to realize face detection. In order to improve the accuracy of face detection, this paper adds three rectangular features on the basis of the original rectangular features (Figure 1), as shown in Figure 2.

In Figure 2, the left rectangle is used to represent the left cheek, the middle rectangle is used to represent the right cheek, and the right rectangle is used to represent the local

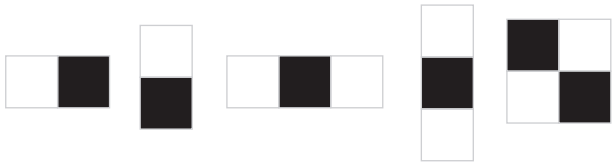

Figure 1: Original rectangular feature.

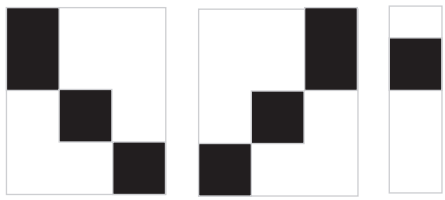

Figure 2: Haar-like feature block proposed.

features of the face. The white part of local features represents the forehead, and the rest represents the eyes.

The improved AdaBoost method obtains the strong classifier $G(x)$ by combining several weak classifiers.

$$f(x) = \sum_{n=1}^{N} e^{a_n G_n(x)},$$
$$G(x) = \operatorname{sign}(f(x)) = \operatorname{sign}\left(\sum_{n=1}^{N} e^{a_n G_n(x)}\right), \tag{1}$$

where a_n represents the coefficient of $G_n(x_i)$, which is how important it is in $G_n(x_i)$.

$$a_n = \frac{1}{2}\log\frac{1-e_n}{e_n}, \tag{2}$$

where e_n represents the error rate on the training set.

$$e_n = \sum_{i}^{M} w_{ni} I(G_n(x_i) \neq y_i), \tag{3}$$

where w_{ni} represents the weight.

Then, the corresponding weights in the training set are constantly updated so that the incorrectly classified samples have increasing weight and the correctly classified samples have decreasing weight. In this way, the training can make the samples that are difficult to classify easily get attention.

3.2. Data Enhancement Algorithm. The Retinex algorithm is based on the consistency of colors and is determined by an object's ability to reflect light. It can strike a balance between dynamic compression, edge image enhancement, and color constancy. At the same time, the lighting and color of objects can be kept consistent, that is, the influence of information transmission between the two is independent. A schematic diagram of Retinex is shown in Figure 3.

The original image is enhanced after illumination estimation and correction. The R and L branches in the above process can be expressed by the following formula:

$$I(x, y) = R(x, y) \cdot L(x, y), \tag{4}$$

where $I(x, y)$ represents the received image information, $R(x, y)$ represents the reflection parameter of the target object in the image information distribution, and $L(x, y)$ represents the irradiation parameter.

In the field of image processing, the principle of image enhancement is often used in order to obtain better adaptive images. Retinex differs from traditional image enhancement algorithms, such as linear and nonlinear transformations, random cropping, and flipping, in that they can only locally enhance certain features of the image.

The Multiscale Retinex (MSR) algorithm is used to enhance the face data image, in order to solve the problem of the complexity of the Retinex method in operation and the decrease of operation speed and to better adapt to the artificial neural network. Gaussian filtering is completed after the face image is processed in batch, and then, the filtering results at different scales are averaged to obtain the best face image. The calculation formula is as follows:

$$r_i(x, y) = \sum_{K=1}^{N} w_k(\log_2(I_i(x, y)) - \log_2(I_i(x, y) * F_k(x, y))), \tag{5}$$

where N represents the number of scale parameters, w_k represents the average weight of the k-th scale, and $F_k(x, y)$ represents the Gaussian filter function on the k-th scale.

$$\sum_{K=1}^{N} w_k = 1,$$
$$F_k(x, y) = \frac{1}{\sqrt{2\pi c_k}}\exp\left(-\frac{x^2 + y^2}{2c_k^2}\right), \tag{6}$$

where c_k represents the calculation coefficient on the k-th scale.

3.3. The Improved DenseNet Network Model. DenseNet is an artificial network with a new connection mode. In the DenseNet network, each layer is connected with all other layers; each layer receives its input from all previous layers and propagates the feature mapping of this layer to all subsequent layers to ensure the maximum transmission of information between the layers of the network. Compared with other neural networks, this network has the advantages of encouraging feature reuse, strengthening feature transfer, reducing the amount of calculation, and alleviating the disappearance of a gradient. It is more suitable for fatigue state detection. Therefore, this paper improves on the basis of DenseNet to improve the accuracy of fatigue state evaluation. The network structure of DenseNet is shown in Figure 4.

Because the correlation between the training features is increased between the layer and layer connections of the network, in the network with dense connections, the similar features generated by the later layer connections are better than those generated by the previous layer connections. The last layer of dense connection often accepts the output of all previous layers as input for aggregation, but there is

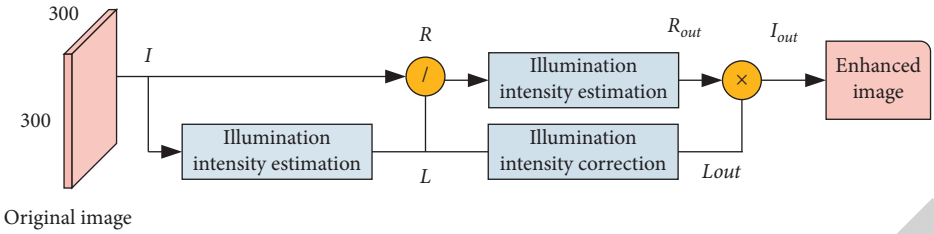

Figure 3: Retinex principle process.

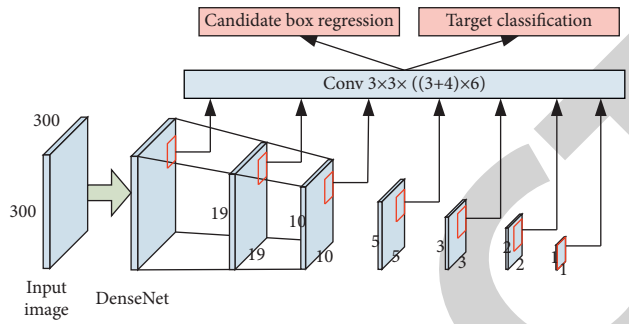

Figure 4: Network structure of DenseNet.

redundant information between these features in the last layer, resulting in the easy loss of feature information in the lower layer.

DenseNet has the defect that feature information is easy to be lost, so it should be improved. The main idea of this paper is to abandon the traditional idea that each layer in DenseNet accepts the output of all previous layers as the input of this layer, in order to reduce the number of interlayer connections. The connection of the first part of the network maintains a dense connection state; the later part is connected to the next layer with only one connection. The structure diagram of the improved new module is shown in Figure 5:

As shown in Figure 5, firstly, 1×1 convolution is used to change their dimensions to 256. For 38×38 sizes, the feature map needs to use a step size of 2 and filter size of 2×2 and downsample it to 19×19. The bilinear interpolation method should be used to upsample the feature graph with a scale smaller than 19×19 to enlarge it to 19×19. They are then concatenated together to form a pixel layer; Batch Norm processing is used to make the activation values of different hierarchical features with the same order of magnitude. Finally, this layer is used as the base layer to generate subsequent connections through the simple stacking of 3×3 convolution blocks.

3.4. Optimization of DenseNet Structure Based on QPSO. Because the velocity of PSO particle has upper limit, its search space is limited. From the perspective of quantum mechanics, QPSO enables the particle to have an uncertain search trajectory, searching in the whole feasible region, but with global convergence. The iterative expression of QPSO algorithm is as follows:

$$\begin{aligned} p_{id}^k &= \varphi_{id}^k \text{pbest}_{id}^k + \left(1 - \varphi_{id}^k\right)\text{gbest}_d^k, \\ \varphi_{id}^k &\sim U(0,1), \\ x_{id}^{k+1} &= p_{id}^k \pm \frac{L_{id}^k}{2} \ln \frac{1}{u_{id}^k}, \\ u_{id}^k &\sim U(0,1), \end{aligned} \tag{7}$$

where x_{id}^{k+1} is the d-dimensional component of the i-th particle position in the k+1-th iteration, φ_{id}^k and u_{id}^k are the random numbers evenly distributed on (0, 1), pbest_{id}^k is the d-dimensional component of the individual optimal position (local optimal value) of particle i in the k-th iteration, and gbest_d^k is the d-dimensional component of the optimal particle position (global optimal value) of all particles in the population.

The update mode of pbest_{id}^k and gbest_d^k in the QPSO algorithm is exactly the same as that of the PSO algorithm.

$$L_{id}^k = 2\alpha \left| x_{id}^k - C_d^k \right|, \tag{8}$$

where α is the compression expansion factor. When α<1.781, the QPSO algorithm converges globally. C_d^k is the average value of the d-dimensional component of its own optimal position gbest_d^k in the search process of all particles in the population.

$$C_d^k = \frac{1}{N} \sum_{i=1}^{N} \text{pbest}_{id}^k, \quad (1 \le d \le M), \tag{9}$$

where N is the population size and M is the particle dimension.

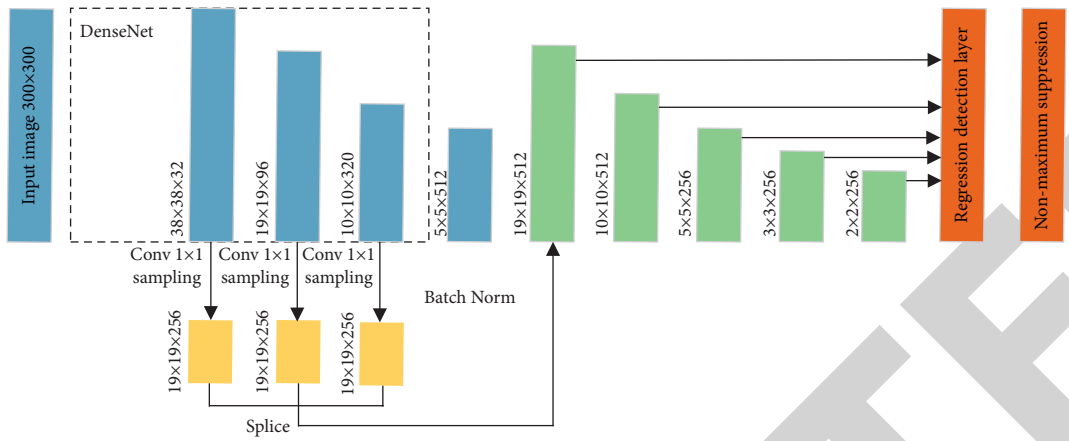

Figure 5: Improved DenseNet network structure.

The flowchart of the QPSO-DenseNet model is shown in Figure 6.

4. Experiment and Analysis

4.1. Experimental Environment and Parameter Setting. The experimental simulation environment includes Inter core i7-8750h, 8 GB memory, and graphics card GTX 1060. The operating system is Windows 10. Deep learning framework is TensorFlow, and we use Microsoft Visual Studio 2010 as the development environment. The maximum number of iterations of QPSO is set to 30, the population size is 10, and the dimension of particles is 11.

4.2. Fatigue Discrimination Parameters.

(1) The parameter PERCLOS is the ratio of the time of eye closure to the time of monitoring. Within a certain period of time, when the number of eye closure frames exceeds 70% or 80%, it can be judged as fatigue. Since the number of frames of the image collected using the camera in a fixed time is unchanged, the PERCLOS value is expressed by the ratio of the number of frames with eyes closed in the video to the total number of frames in the video during this period, which can be expressed by the following formula:

$$\text{PERCLOS} = \frac{\text{eyes closed frames}}{\text{total frames in detection period}} \times 100\%. \tag{10}$$

(2) The parameter BF is the number of blinks per unit time. There are two types of blinking: protective blinking in response to external stimuli and human involuntary behavior. Normal nonfatigue people will blink quickly; especially when you are energetic, the BF value is 2–4 times per second and the duration of each blink is short about 0.25–0.3 seconds; when people are tired, their blinking speed will slow down, BF will decrease, and the duration will be prolonged after each eye closure. In order to study the BF characteristics under fatigue state, 10 sample data under different fatigue states are randomly selected from the dataset for analysis and the mean and standard deviation under nonfatigue state and fatigue state with time windows of 20 s and 40 s are calculated, respectively, as shown in Table 1.

It can be seen that BF is significantly different in the 20 s and 40 s time windows, so BF can be used as the detection parameter of fatigue driving. Based on the above experimental analysis, the CAS_PEAL dataset [28] was selected, and each face in the dataset had 27 different posture images. A partial example of the CAS_PEAL dataset is shown in Figure 7.

Two parameters, PERCLOS and BF, were used to discriminate fatigue. w was used to represent the proportion of PERCLOS parameter in the discrimination (the proportion of BF parameter was $1 - w$). Figure 8 shows the accuracy of the PERCLOS parameter discriminating fatigue with different proportions.

It can be seen from Figure 8 that when $w = 1$, that is, only the PERCLOS parameter is used to distinguish fatigue, the accuracy rate is 92.4%. When $w = 0$, that is, only the BF parameter is used to distinguish fatigue, the accuracy rate is 82%. When $w = 0.6$, the accuracy is 91%. It can be concluded that the comprehensive detection result of PERCLOS and BF is better than that of a single parameter.

4.3. Comparative Analysis of Experimental Results under Different Loss Functions. In this experiment, the artificial neural network model was used to conduct experiments on the CAS_PEAL and self-built datasets and the accuracy of fatigue state discrimination was compared horizontally. During the test, the test set randomly included images with stronger blocking effects such as environment, light, and angle. In order to verify the validity and correctness of the proposed improved loss function, the settings of the loss function are constantly changed under the condition that other parameters in the network model remain unchanged, so as to test the performance of different loss functions in the network, as shown in Table 2.

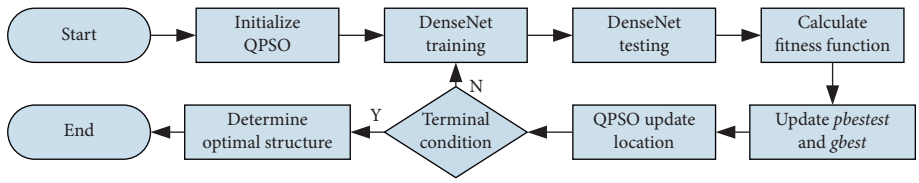

Figure 6: Flowchart of the QPSO-DenseNet model.

Table 1: Analysis table of blink frequency in nonfatigue state and fatigue state.

Time window (s)	Not fatigued		Fatigued	
	Mean value	Standard deviation	Mean value	Standard deviation
20	15.10	5.97	15.46	5.65
40	15.10	3.65	15.46	3.64

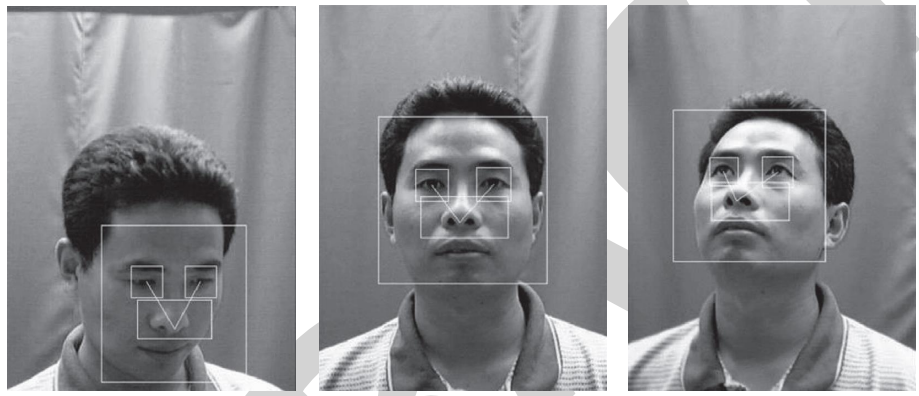

Figure 7: Partial example of the CAS_PEAL dataset.

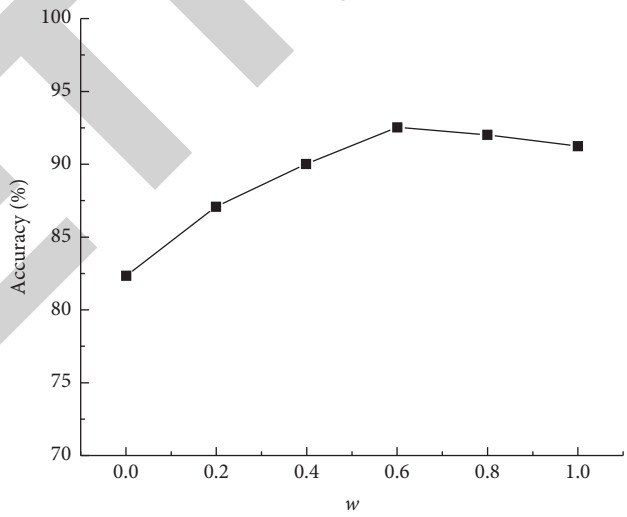

Figure 8: The accuracy rate varies with the parameter ratio.

As can be seen from Table 2, Softmax loss function has a good performance in both the original dataset and the dataset containing affected images. Therefore, Softmax loss function is uniformly used in subsequent experiments.

4.4. Comparative Analysis of Experimental Results under Different Connection Modes. In order to verify the correctness and effectiveness of the improved connection mode in this paper, the network with unchanged connection mode and the network with improved connection mode in this experiment are tested and compared on different datasets, and the results are shown in Table 3.

As can be seen from Table 3, in terms of detection accuracy, the network with improved connection mode in this

Table 2: Correct recognition rate under different loss functions.

Loss function	Original dataset	Datasets with affected images
Hinge loss	0.866	0.821
Softmax loss	**0.891**	**0.844**
Square loss	0.882	0.779
Exponential loss	0.831	0.798
Smooth L1 loss	0.843	0.801

Table 3: The verification accuracy of different networks.

Dataset	Accuracy of detection under different connection modes		Average time consumption under different connection modes (s)	
	Original link mode	Improved link mode	Original link mode	Improved link mode
CAS_PEAL	0.891	**0.897**	0.52	**0.47**
Self-built dataset	0.837	**0.852**	0.73	**0.65**

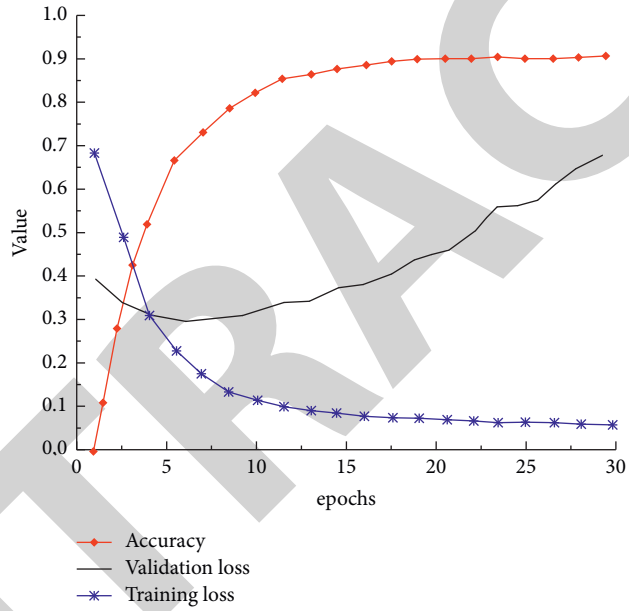

Figure 9: Network training process diagram.

Table 4: Accuracy of detection under different datasets.

	DenseNet	QPSO-DenseNet
CAS_PEAL	0.891	**0.921**
Self-built dataset	0.837	**0.872**
CAS_PEAL + self-built datasets	0.781	**0.813**

The bold values given in all tables indicate better performance.

Table 5: Comparison of accuracy of different models.

	CNN	PSO-CNN	QPSO-DenseNet
CAS_PEAL	0.886	0.903	**0.921**
Self-built dataset	0.824	0.865	**0.872**
CAS_PEAL + self-built datasets	0.767	0.809	**0.813**

paper has a better performance in CAS_PEAL and self-built datasets. In terms of average time consumption, the network with improved connection mode in this paper has low time consumption in both datasets. The results show that the improved network not only improves the detection accuracy but also reduces time consumption.

4.5. Comparative Analysis of Comprehensive Experimental Results. In order to verify the overall efficiency of the QPSO-DenseNet model, the detection accuracy curve and loss function curve with the change of training times were plotted. It can be seen from the curve that the accuracy rate changes with the training times, when it is close to 30 epochs, the accuracy rate is basically stable, and the loss rate also tends to be stable. The network training process is shown in Figure 9.

The accuracy results of the QPSO-DenseNet model and the original DenseNet model on CAS_PEAL and self-built datasets are shown in Table 4.

It can be seen that the accuracy of the QPSO-DenseNet model is higher than that of the original DenseNet model in a comprehensive view, no matter in a certain dataset or two datasets. In order to fully verify the advancement of the proposed model, comparison with the CNN and PSO-CNN models was carried out under the same experimental conditions. The accuracy comparison results are shown in Table 5.

It can be seen from Table 5 that the QPSO-DenseNet model in this paper is superior to the CNN and PSO-CNN models in terms of final detection accuracy. When QPSO-DenseNet trains face images, feature reuse produces a network model with easy training and a high parameter efficiency. By connecting the eye feature maps learned in different layers, the input changes of subsequent layers are increased and the efficiency is improved. This is the main reason why the proposed model is superior to other models. From the above results, it is feasible to use the QPSO-DenseNet model to judge the eye state to describe the fatigue state of students in class.

5. Conclusions

In this paper, based on the traditional DenseNet, an improved DenseNet network framework is constructed by reducing the number of redundant connections and the DenseNet structure is optimized by QPSO. Firstly, experiments are carried out for different loss functions and structures with reduced connection numbers, and the detection accuracy and time consumption are analyzed and compared on different datasets. Finally, the QPSO-DenseNet model was compared with CNN and PSO-CNN models, and the experimental results showed that the QPSO-DenseNet showed a good detection effect.

Data Availability

The experimental data used to support the findings of this study are available from the corresponding author upon request.

Conflicts of Interest

The authors declare that they have no conflicts of interest regarding the present study.

References

[1] Y. Jiang and Y. Wang, "Evaluation of teaching quality of public physical education in colleges based on the fuzzy evaluation theory," *Journal of Computational and Theoretical Nanoscience*, vol. 13, no. 12, pp. 9848–9851, 2016.

[2] J. Cheng and Y. Xiong, "The quality evaluation of classroom teaching based on FOA-GRNN," *Procedia Computer Science*, vol. 107, pp. 355–360, 2017.

[3] Q. Jian, "Multimedia teaching quality evaluation system in colleges based on genetic algorithm and social computing approach," *IEEE Access*, vol. 7, pp. 183790–183799, 2019.

[4] K. Dong, D. Chu, K. Wang, L. Guo, and S. Gu, "A classroom teaching quality evaluation system for the master of software engineering in China based on engineering education accreditation," *Computer Education*, vol. 288, no. 12, pp. 125–130, 2018.

[5] A. Abdelhadi and M. Nurunnabi, "Engineering student evaluation of teaching quality in Saudi arabia," *International Journal of Engineering Education*, vol. 35, no. 1A, pp. 262–272, 2019.

[6] M. L. Rocca, M. L. Parrella, I. Primerano, I. Sulis, and M. P. Vitale, "An integrated strategy for the analysis of student evaluation of teaching: from descriptive measures to explanatory models," *Quality and Quantity*, vol. 51, no. 2, pp. 1–17, 2016.

[7] S. Liqiong, Y. Jing, J. Xiaoyan, H. Luoya, S. Shoimai, and Z. Yan, "Based on Delphi method and Analytic Hierarchy Process to construct the Evaluation Index system of nursing simulation teaching quality," *Nurse Education Today*, vol. 79, pp. 67–73, 2019.

[8] K. Dreiling, D. Montano, H. Poinstingl et al., "Evaluation in Undergraduate Medical Education: Conceptualizing and Validating a Novel Questionnaire for Assessing the Quality of Bedside teaching," *Medical Teacher*, vol. 39, pp. 1–8, 2017.

[9] A. Buczak and E. Guven, "A survey of data mining and machine learning methods for cyber security intrusion detection," *IEEE Communications Surveys & Tutorials*, vol. 18, no. 2, pp. 1153–1176, 2017.

[10] M. Raissi and G. E. Karniadakis, "Hidden physics models: machine learning of nonlinear partial differential equations," *Journal of Computational Physics*, vol. 357, pp. 125–141, 2018.

[11] C. Voyant, G. Notton, and S. Kalogirou, "Machine learning methods for solar radiation forecasting: a review," *Renewable Energy*, vol. 105, no. 5, pp. 569–582, 2017.

[12] M. P. Pound, J. A. Atkinson, A. J. Townsend et al., "Deep Machine Learning provides state-of-the-art performance in image-based plant phenotyping," *GigaScience*, vol. 6, no. 10, pp. 1–10, 2018.

[13] I. Kavakiotis, O. Tsave, A. Salifoglou, N. Magalveras, L. Vaglavas, and L. Chouvarda, "Machine learning and data mining methods in diabetes research," *Computational and Structural Biotechnology Journal*, vol. 15, no. C, pp. 104–116, 2017.

[14] S. Liu, X. Wang, M. Liu, and J. Zhu, "Towards better analysis of machine learning models: a visual analytics perspective," *Visual Informatics*, vol. 1, no. 1, pp. 48–56, 2017.

[15] M. Kohli, L. M. Prevedello, R. W. Filice, and J. R. Geis, "Implementing machine learning in radiology practice and research," *American Journal of Roentgenology*, vol. 208, no. 4, pp. 1–7, 2017.

[16] X. Lin, X. Wang, and L. Li, "Intelligent detection of edge inconsistency for mechanical workpiece by machine vision

with deep learning and variable geometry model," *Applied Intelligence*, vol. 50, no. 7, pp. 2105–2119, 2020.

[17] T. Kim, I. Y. Jung, and Y. C. Hu, "Automatic, location-privacy preserving dashcam video sharing using blockchain and deep learning," *Human-centric Computing and Information Sciences*, vol. 10, no. 1, pp. 1–23, 2020.

[18] A. S. Devi, G. Maragatham, K. Boopathi, and A. G. Rangaraj, "Hourly day-ahead wind power forecasting with the EEMD-CSO-LSTM-EFG deep learning technique," *Soft Computing*, vol. 24, no. 16, pp. 12391–12411, 2020.

[19] S. Park, Y. Jeong, and H. S. Kim, "Multi-resolution DenseNet based acoustic models for reverberant speech recognition," *Phonetics and Speech Sciences*, vol. 10, no. 1, pp. 33–38, 2018.

[20] X. Zhang, J. Zhang, Y. Hu, T. Tang, J. Yang, and Y. Zhang, "Structural damage recognition based on the finite element method and quantum particle swarm optimization algorithm," *IEEE Access*, vol. 8, pp. 184785–184792, 2020.

[21] H. Luo, T. Qiu, C. Liu, and P. Hunga, "Research on fatigue driving detection using forehead EEG based on adaptive multi-scale entropy," *Biomedical Signal Processing and Control*, vol. 51, pp. 50–58, 2019.

[22] F. Wang, S. C. Wu, and S. L. Liu, "Driving fatigue detection based on EEG deep transfer learning," *Journal of Electronics and Information Technology*, vol. 41, no. 9, pp. 2264–2272, 2019.

[23] C. Qian, Z. Wang, L. Zuo, C. Li, and H. Liu, "Design and research of anti-fatigue driving system based on human eye recognition," *Journal of Jilin University (Earth Science Edition)*, vol. 34, no. 4, pp. 522–527, 2016.

[24] F. You, Y. H. Li, L. Huang, K. Chen, R. H. Zhang, and J. M. Xu, "Monitoring drivers' sleepy status at night based on machine vision," *Multimedia Tools and Applications*, vol. 76, no. 13, pp. 14869–14886, 2017.

[25] W. Guo, B. Zhang, L. Xia, S. Shi, X. Zhang, and J. She, "Driver drowsiness detection model identification with bayesian network structure learning method," in *Proceedings of the Control & Decision Conference*, pp. 131–136, IEEE, Yinchuan, China, May 2016.

[26] S. Bao, S. Ma, and C. Yang, "Multi-scale retinex-based contrast enhancement method for preserving the naturalness of color image," *Optical Review*, vol. 27, no. 6, pp. 475–485, 2020.

[27] G. Antipov, M. Baccouche, S. A. Berrani, and J. L. Deglay, "Effective training of convolutional neural networks for face-based gender and age prediction," *Pattern Recognition*, vol. 72, pp. 15–26, 2017.

[28] A. A. Elngar and M. Kayed, "Vehicle security systems using face recognition based on internet of things," *Open Computer Science*, vol. 10, no. 1, pp. 17–29, 2020.